# Scale invariance and criticality in nuclear spectra

E. Landa, I. Morales, C. Hernández, J.C. López Vieyra, and A. Frank
*Instituto de Ciencias Nucleares, Universidad Nacional Autónoma de México,*
*Apartado Postal 70-543, México, D.F. 04510 México.*

V. Velázquez
*Facultad de Ciencias, Universidad Nacional Autónoma de México,*
*México, D.F. 04510 México.*

Recibido el 15 de abril de 2008; aceptado el 9 de mayo de 2008

A Detrended Fluctuation Analysis (DFA) method is applied to investigate the scaling properties of the energy fluctuations in the spectrum of $^{48}$Ca obtained with (a) a large realistic shell model calculation (ANTOINE code) and (b) with a random shell model (TBRE) calculation. We compare the scale invariant properties of the energy fluctuations with similar analyses applied to the RMT ensembles GOE and GDE. A comparison with the related power spectra calculations is made. The possible consequences of these results are discussed.

*Keywords:* Quantum chaos; scale invariance; TBRE; DFA.

Se aplica el método DFA (Detrended Fluctuation Analysis) para investigar las propiedades de escalamiento de las fluctuaciones de la energía en el espectro del $^{48}$Ca obtenido con (a) un cálculo del modelo de capas realista (codigo ANTOINE) y con (b) un cálculo del modelo de capas aleatorio (TBRE). Comparamos las propiedades invariantes de escala de las fluctuaciones de energía con análisis similares aplicados a ensembles GOE y GDE de la teoría de matrices aleatorias (RMT). Se hace una comparación con cálculos relacionados de espectro de potencias. Se discute las posibles consecuencias de esos resultados.

*Descriptores:* Caos cuántico; invariancia de escala; TBRE; DFA.

PACS: 05.45.Mt;24.60.Lz;52.25.Gj;74.40.+k;89.75.Da

## 1. Introduction

Our present knowledge of highly excited states in heavy nuclei is based on the connection with the eigenvalues of random (chaotic) hamiltonians. On the scale of the mean level spacing, the spectra of complex nuclei are statistically described by Random Matrix Theory (RMT) [1]. This notion was introduced by E. Wigner in the 1950s [2]. In particular, the probability distribution $P(s)$ of the nearest-neighbor spacing $s$ agrees with the Wigner surmise[i]

$$P(s) = \pi/2\, s e^{-\pi\, s^2/4}$$

of RMT. Furthermore, the Bohigas-Giannoni-Schmit-conjecture [3] establishes that quantum systems whose classical analogs are chaotic, have a nearest-neighbor spacing probability distribution given by RMT, whereas for systems whose classical counterparts are integrable, the nearest-neighbor spacings are described by a Poisson distribution [4] $P(s) = e^{-s}$. Thus, a widely accepted criterion for a signature of quantum chaos is usually made in terms of the form of $P(s)$. Intermediate situations are analyzed by means of interpolated distributions (see *e.g.* Refs 5 and 6).

Classical chaos, on the other hand, is a better understood non-linear phenomenon, which gives rise to an *unpredictable* time-evolution of the corresponding dynamical systems. In particular, it is characterized by an intrinsic instability in the orbits due to a high sensitivity to initial conditions. So, instead of trying to make a precise prediction of individual trajectories the aim of the theory of chaos is a description of the space of possible trajectories and the evaluation of average quantities on this space. In general, the dynamical instability of the orbits in a chaotic system is accompanied by the occurrence of strange attractors with a fractal structure in phase space (*e.g.* in the Lorenz model -see Fig. 1). The origin of this fractal structure is related to the existence of a rigid *tree* of periodic orbits (*cycles*) of increasing lengths and self-similar structure [7]. The relation between the structure of periodic orbits in phase space and RMT is established by Gutzwiller trace formula [8]. Thus, at the quantum level we would hope to find a signature of the fractality in the phase space in the form of a scale invariance, or, in other words, to identify the same kind of signature (or symmetry) in the quantum regime[ii]

The notion of scale invariance appears in many different phenomena. For example, in second order phase transitions, it appears near the so called *critical points* where some physical quantities obey a power law behavior. In paricular, the correlation lenght[iii] $\xi$ behaves like $\xi \sim |T - T_{crit}|^{-\nu}$, with $\nu$ being the corresponding *critical exponent*. At the critical temperature the correlation lenght $\xi$ diverges and the system has no characteristic scale, *i.e.* the system becomes scale invariant, and the correlation function behaves as $\Gamma(r) \sim r^{-p}$.

Power law behavior has been observed in the study of chaotic time series, for example in the problem of a dripping faucet [9], in heartbeat dynamics [10] and in many other phenomena. Recently, it was found that the power spectrum of the fluctuations of the eigenvalues of RMT ensembles and nuclear shell (TBRE) model calculations exhibit a power law behavior $\sim 1/f$ (with $f$ being the frequency), whereas, for the case of integrable systems it was found that the corre-

sponding power spectrum behaves as $\sim 1/f^2$ (see Ref. 11). Thus, in the case of a system with a (parameter-dependent) transition from a regular to a chaotic regime, like the hydrogen atom in an external magnetic field, we would expect to have a power spectrum $\sim 1/f^2$ associated with the energy fluctuations at small magnetic fields, and $\sim 1/f$ for magnetic fields $B \gtrsim 1$ (in atomic units). To our knowledge, the dependence of this transition on the external magnetic field intensity has not been well understood so far. This problem will be studied elsewhere.

The purpose of the present paper is to begin a study of the self-similar (or fractal) properties of the energy fluctuations in the spectrum of quantum chaotic systems. As a concrete system we study the energy fluctuations in the spectrum of $^{48}$Ca, obtained with (a) shell model calculations with a *realistic* interaction, and (b) with random shell model calculations (TBRE) both in the full fp shell. Large shell calculations are considered to exhibit the chaotic behavior found in actual experimental spectra (see *e.g.* Ref. 23 and references therein). We also carry out a comparison with the corresponding behavior of the energy fluctuations in the RMT ensembles GOE and GDE. We shall also use a recently introduced notion based on the analogy between energy fluctuations of chaotic hamiltonians and chaotic time-series, and apply the method of *detrended fluctuation analysis* (DFA) [15], which is designed to study the hidden fractal properties of time series found in many natural phenomena.

## 2. Fractality and $1/f$ scale invariance

The concept of a fractal is associated with geometrical objects satisfying two criteria: self similarity and fractional dimensionality. Self similarity means that an object is composed of sub-units and sub-sub-units on multiple levels that (statistically) resemble the structure of the whole object. A related property is scale invariance which can be thought of as self-similarity on all scales. Thus, a fractal structure lacks any characteristic length scale. This fractal structure is seen, *e.g.*, in the Lorenz attractor Fig. 1.

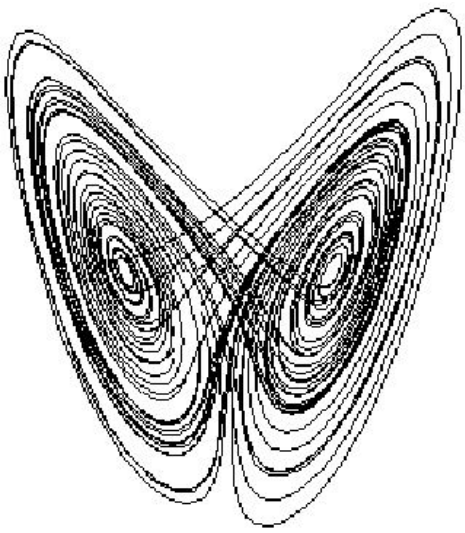

FIGURE 1. Lorenz strange attractor having a fractal (Hausdorff) dimension $\sim 2.06$.

The $1/f$ behavior of the power spectrum found in quantum fluctuations of the spectra of random hamiltonians [11,17] suggests that full quantum chaos can be associated with a particular class of scale invariance. Namely, a scale invariance for which the auto-correlation function becomes (approximately) scale independent. Such situation occurs for a power spectrum with a power-law (scale invariant) behavior $\sim 1/f^\beta$ at the *critical* value $\beta = 1$. A demonstration in the continuum case is the following: suppose that the power spectrum[iv] of a given time series has a $1/f$ behavior, *i.e.*

$$\mathcal{S}(f) = 1/f\,. \tag{1}$$

Since the Fourier Transform of the power spectrum is identical to the autocorrelation function $\mathcal{C}(\tau)$ (Wiener-Khinchin Theorem[v]) we have:

$$\mathcal{C}(\tau) = \mathcal{F}^{-1}(\mathcal{S}(f)) = \mathcal{F}^{-1}(1/f)\,. \tag{2}$$

Now, if we make an arbitrary scale transformation in the *time* domain (*i.e.* $\tau \to a\tau$, $a \in \mathbb{R}^+$) we have

$$\mathcal{C}(a\tau) = \mathcal{F}^{-1}\left(\frac{1}{a}\left(\mathcal{S}(f/a)\right)\right) = \mathcal{F}^{-1}\left(\frac{1}{a}\times\frac{a}{f}\right)\,. \tag{3}$$

Thus

$$\mathcal{C}(a\tau) = \mathcal{C}(\tau)\,. \tag{4}$$

Here, we have used the scaling property of Fourier Transforms, which is strictly valid only in the continuum case. For discrete time series, there are other tools for studying their scale invariant properties, including the DFA method [15] (see below). In fact, $1/f$ behavior (referred to as flicker or $1/f$ *noise*) occurs in many physical, biological and economic systems, meteorological data series, the electromagnetic radiation output of some astronomical bodies, and in almost all electronic devices. In biological systems, it is present in heart beat rhythms and the statistics of DNA sequences. In financial systems it is often referred to as a long memory effect. There are even claims that almost all musical melodies, when each successive note is plotted on a scale of pitches, will tend towards a $1/f$ noise spectrum.

## 3. Spectrum fluctuations as time-series

The fluctuations in a quantum spectrum are obtained by an unfolding procedure, *i.e.*, by substracting the gross features of the spectrum which can be modeled by a smooth function. In essence, this procedure consists in mapping the spectrum[vi] $E_i$ into a dimensionless spectrum $\epsilon_i$, having a mean level density of 1:

$$E_i \to \epsilon_i \equiv \bar{N}(E_i)\,, \quad (i = 1, \ldots N)\,. \tag{5}$$

where $\bar{N}(E_i)$ is a smooth function fit[vii] of the staircase-like cumulative density function $N(E_i)$ (see *e.g.* Ref. 8). In particular, the nearest neighbor spacing (NNS) is calculated as $s_i = \epsilon_{i+1} - \epsilon_i\,, i = 1, \ldots N-1$, and $\langle s\rangle = 1$. The spectrum fluctuations can be defined by the quantity

$$\delta_n = \sum_{i=1}^{n}(s_i - \langle s\rangle) = [\epsilon_{n+1} - \epsilon_1] - n\langle s\rangle\,. \qquad (6)$$

The stochastic discrete function $\delta_n$ measures the deviations of the distance between the first and the $(n+1)$-th unfolded states, with respect to the corresponding distance in a uniform (equally spaced) sequence having a unit level distance $\langle s\rangle = 1$. The sequence (6) can be formally interpreted as a discrete "time series" (see *e.g.* Ref. 11). In order to understand the scaling properties of the fluctuations (6), we use the detrended fluctuation analysis (see below).

A standard measure for the deviation from equal spacing is the Dyson-Metha *rigidity* function [16]

$$\Delta_3(L;\alpha) = \frac{1}{L}\mathrm{Min}_{A,B}\int_{\alpha}^{\alpha+L}\left[N(E) - A\,E - B\right]^2 dE\,, \quad (7)$$

where $A, B$ give the best local fit to $N(E)$ in the observation window $\alpha \le E \le \alpha + L$. The harmonic oscillator corresponds to the minimum value $\Delta_3 = 1/12$ (maximum rigidity), while a completely random (uncorrelated) spectrum with a Poisson distribution has an average (over $\alpha$) $\overline{\Delta}_3(L) = L/15$ (see *e.g.* Ref. 8). The case of a GOE spectrum with a Wigner-like NNS probability distribution is an intermediate case and the rigidity function has the form $\overline{\Delta}_3(L) = 1/\pi^2(\log L - 0.0687)$. It has been shown in Ref. 17 that the rigidity function (7) is related to the DFA method. In particular, Santhanam *et al.* [17] have applied the DFA method to RMT ensembles as well as to the spectra of heavy atoms.

## 4. Detrended fluctuation analysis (DFA)

DFA is a method which allows the investigation of long range correlations and scaling properties in a random time series. It was first introduced in studies of DNA chains [15]. In the following we make a brief description of the DFA method (for more details we refer the reader to the original paper [15]).

A time series $\delta(t)$ is self similar if the statistical properties of the full time series and the statistical properties of any rescaled subinterval of it, satisfy the scaling relation

$$\delta(t) \overset{\text{PDF}}{=} a^{\alpha}\delta\left(\frac{t}{a}\right)\,, \qquad (8)$$

where $a$ is the scale factor in the *time* axis ($a^{\alpha}$ is the corresponding vertical scaling factor). The exponent $\alpha$ in Ref. 8 is defined as the self-similarity parameter. We emphasize that the equality in Ref. 8 is understood as indicating the *same* probability distributions (PDF).

Let $\delta(i)$, $i = 1 \ldots N$ be a time series. The DFA analysis of $\delta(i)$ begins by defining an integrated time series

$$\psi(n) = \sum_{i=1}^{n}[\delta(i) - \langle\delta\rangle]\,, \qquad (9)$$

with $\langle\delta\rangle$ being the average (expectation value) of $\delta$. Then the integrated time series is divided into boxes of equal length $\ell$, where a linear[viii] least-squares fit $\psi_\ell(n)$ (trend) is made. The difference (r.m.s.) between the integrated time series and the fit is measured by the *detrended fluctuation*

$$F(\ell) \equiv \sqrt{\frac{1}{N}\sum_{n=1}^{N}[\psi(n) - \psi_\ell(n)]^2}\,. \qquad (10)$$

This fluctuation can be calculated for all scale factors (or box sizes). In a log-log plot, a linear relationship between the fluctuation and the box size will indicate a scaling (power law) behavior. In this case the slope $\alpha_{DFA}$ in the $\log[F(\ell)]$ vs $\log[\ell]$ plot can be used to characterize the scaling properties (8) of the original time series since $\alpha = \alpha_{DFA}$ in Ref. 8. As an example, if there is no correlation among the points in the original time series $\delta(i)$, *i.e.* the autocorrelation function[ix] $\mathcal{C}(\tau) \equiv 0$, for any time-lag $\tau \neq 0$, the time series behaves as white noise and the integrated time series $\psi(n)$ corresponds to a random walk characterized by $\alpha_{DFA} = 0.5$ (see [18]). Time series with short range (exponentially decaying) correlations $\mathcal{C}(\tau) \sim e^{-\tau/\tau_0}$, $\tau_0$ being the characteristic scale, are also characterized by $\alpha_{DFA} \simeq 0.5$ although some deviations from $\alpha_{DFA} \simeq 0.5$ may occur for small window sizes. Of special interest are the so called *persistent* (long time memory) time series for which the autocorrelation function has a power-law behavior $\mathcal{C}(\tau) \sim \tau^{-\gamma}$. They are characterized by values $0.5 < \alpha_{DFA} < 1.0$, the relationship between $\gamma$ and $\alpha_{DFA}$ being $\gamma = 2 - 2\alpha_{DFA}$. The power spectrum of the corresponding time-series also displays a power-law (scale invariant) behavior $S(f) \sim 1/f^{\beta}$ with $\beta = 1 - \gamma = 2\alpha_{DFA} - 1$. In particular, for time series with $1/f$-noise ($\beta = 1$) $\alpha_{DFA} = 1$ (see *e.g.* Ref. 19).

## 5. Results

We have applied the DFA method and performed a spectral analysis to the energy fluctuations in the spectrum of $^{48}\mathrm{Ca}$. For comparison purposes we have also applied the analysis to the case of RMT ensembles GOE and GDE. In all cases the unfolding (5) to the spectrum was done (for simplicity) with a polynomial fit. After a careful analysis, a degree-7 polynomial fit was used in each case[x] However, the unfolding is a delicate procedure when defining the energy fluctuations [11]. It can lead to wrong conclusions when not properly done. In particular, the results are rather sensitive to the degree of the polynomial in a polynomial fit to $\bar{N}(E_i)$ Eq. (5). This fact has been discussed in TBRE calculations in Ref. 13. In our analysis we have suitably removed the tails of

the spectrum to avoid a strong dependencies of the results in the polynomial fit.

In the present calculations we have used the *dfa* C-code (translation of Peng's original fortran code [20]) with a linear detrending option. The minimal box size used was 4, and the maximal box size was $N/4$, with $N$ the number of points in the time series. The results of the analysis are presented in the following paragraphs.

### 5.1. Realistic shell model calculations

Large shell model calculations with realistic interactions (KB3) [21] were performed in the full fp shell for $^{48}$Ca in the subspaces $J^\pi = 0^+, 1^+, \ldots 8^+$ by means of the ANTOINE code [24]. Within each subspace we calculated the energy fluctuations following the definition (6) and applied a linear DFA analysis. The value of the self-similarity parameter $\alpha$ are found to be very close to 1, the largest deviations being $\sim 10\%$). The energy fluctuations represented by the time series $\delta_n$ and its integrated form $\psi_n$, are shown in Figs. 2a and 3a, respectively, for the case of the subspace $J^\pi = 0^+$. The behavior shown in these figures is typical of all cases studied with shell model calculations with realistic interactions.

Figure 4a shows the results of the DFA analysis for the case of the $J^\pi = 0^+$ subspace. This case is particularly interesting since this subspace contains only 347 energy levels. It is quite remarkable that, even in this case, the trend of the fluctuations is well approximated by a linear scaling in the log-log plot in the whole domain of window sizes giving a self-similarity parameter $\alpha = 0.97$. Larger calculations show even better linear scalings. The results of the DFA analysis are summarized in Table I.

An $\alpha$ parameter close to 1 indicates an almost perfect non-trivial scale invariance. Using the relation $\beta = 2\alpha_{DFA} - 1$, we conclude that the power spectrum exhibits a very approximate $1/f$ behavior. This is confirmed by the corresponding power spectrum calculations, shown in Fig. 5a, where we find an exponent $\beta = 1.008$. The power spectrum depicted in Fig. 5a shows the typical behavior in all shell model calculations with realistic interactions: there is a rather large spread in the Fourier amplitudes from a linear scaling.

TABLE I. Self similarity parameter $\alpha$ obtained using a linear DFA method and the $\beta$ exponent in the power spectrum of the energy fluctuations in the shell model calculations of $^{48}$Ca with realistic interactions in different subspaces $J^\pi$. The dimension $N$ of each subspace is also shown.

| $^{48}$Ca | | | |
|---|---|---|---|
| $J^\pi$ | $\alpha$ | $\beta$ | $N$ |
| $0^+$ | 0.969 | 1.008 | 347 |
| $1^+$ | 0.998 | 1.090 | 880 |
| $2^+$ | 1.013 | 1.046 | 1390 |
| $3^+$ | 1.020 | 1.183 | 1627 |
| $4^+$ | 0.985 | 1.127 | 1755 |
| $5^+$ | 0.916 | 1.198 | 1617 |
| $6^+$ | 1.077 | 1.137 | 1426 |
| $7^+$ | 1.095 | 1.180 | 1095 |
| $8^+$ | 0.964 | 1.031 | 808 |

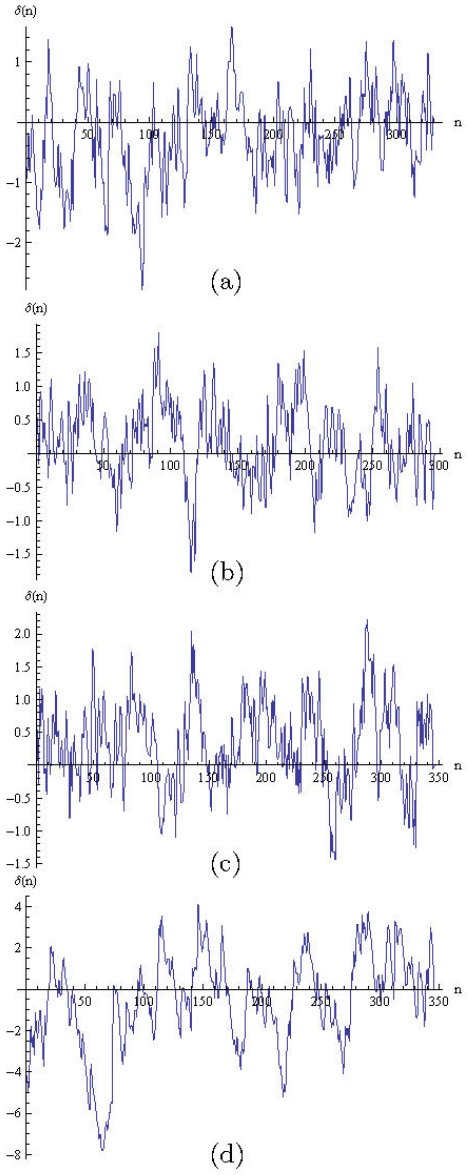


FIGURE 2. Time series $\delta_n$ of the energy fluctuations in a shell model calculation of the spectrum of $^{48}$Ca ($J^\pi = 0^+$ states) with (a) realistic interactions, (b) with random interactions (TBRE), and with RMT ensembles (c) GOE and (d) GDE. For the later the same dimension as for the $J^\pi = 0^+$ subspace was used. The *time* (horizontal) axis represents the index of the ordered unfolded (dimensionless) energy $\epsilon_n$ and the vertical axis represents the corresponding energy fluctuation $\delta_n$ *i.e.* the difference of the $n$-th unfolded energy $\epsilon_n$ with respect to the $n$-th energy level in an equally spaced spectrum with unit energy distance. Notice that the scale for the fluctuations in GDE is about 4 times larger than for the shell model calculations.

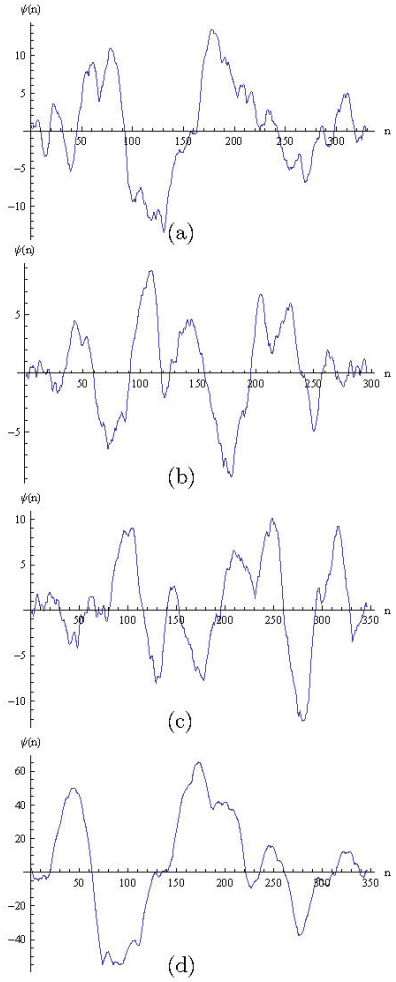


FIGURE 3. Integrated time series $\psi_n$ (Eq. (9)) for the energy fluctuations in shell model calculation of the spectrum corresponding to $^{48}$Ca ($J^\pi = 0^+$ states) with (a) a realistic interaction, (b) with random interactions (TBRE), and with RMT ensembles (c) GOE and (d) GDE. For the cases of GOE and GDE the same dimension as for the $J^\pi = 0^+$ subspace was used. The *time* (horizontal) axis represents the index of the ordered unfolded (dimensionless) energy $\epsilon_n$ and the vertical one the corresponding integrated energy fluctuation $\psi_n$. Notice that the scale for the fluctuations in GDE is about 6 times larger than for the shell model calculations.

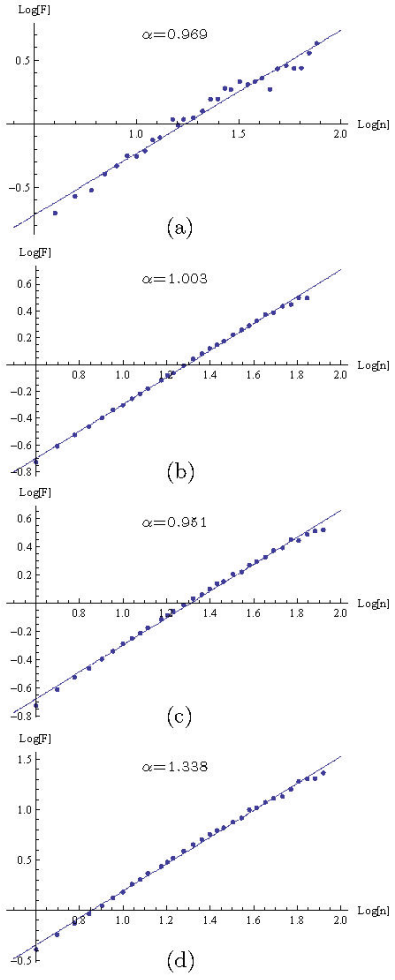


FIGURE 4. Integrated time series $\psi_n$ (Eq. (9)) for the energy fluctuations in shell model calculation corresponding to the spectrum of $^{48}$Ca ($J^\pi = 0^+$ states) with (a) a realistic interaction, (b) with random interactions (TBRE), and with RMT ensembles (c) GOE and (d) GDE. For the later the same dimension as for the $J^\pi = 0^+$ subspace was used. The *time* (horizontal) axis represents the index of the ordered unfolded (dimensionless) energy $\epsilon_n$ and the vertical one the corresponding integrated energy fluctuation $\psi_n$.

The observed spreading is seen independently of the size of the spectrum subspace. We find in all cases that the DFA method is a more robust procedure than the direct calculation of spectral power when analyzing actual experimental data.

### 5.2. TBRE shell calculations

In the present study we have also applied the DFA method to the energy fluctuations of the Two Body Random Ensemble (TBRE) [22] shell model calculations for $^{48}$Ca in the subspace $J^\pi = 0^+$. For this calculations we have used 25 sets of energy levels.

The energy fluctuations represented by the time series $\delta_n$ and its integrated form $\psi_n$ are shown in Figs. 2b and 3b, respectively. The self similarity parameter was calculated by an averaging procedure over the DFA results, and it was found to be $\alpha = 1.01$. This value is very similar to the value of the self similarity parameter obtained in the case of realistic calculations (see Table I). Figure 4b shows the averaged results of the DFA analysis. The linear behavior of these results is very striking. Only for very large window sizes ($n \simeq N/4 \simeq 87$) we can see a slight deviation from linearity. Since the present analysis was done for the case $J^\pi = 0^+$ which has the smallest dimensionality in the fp shell model calculations, it is

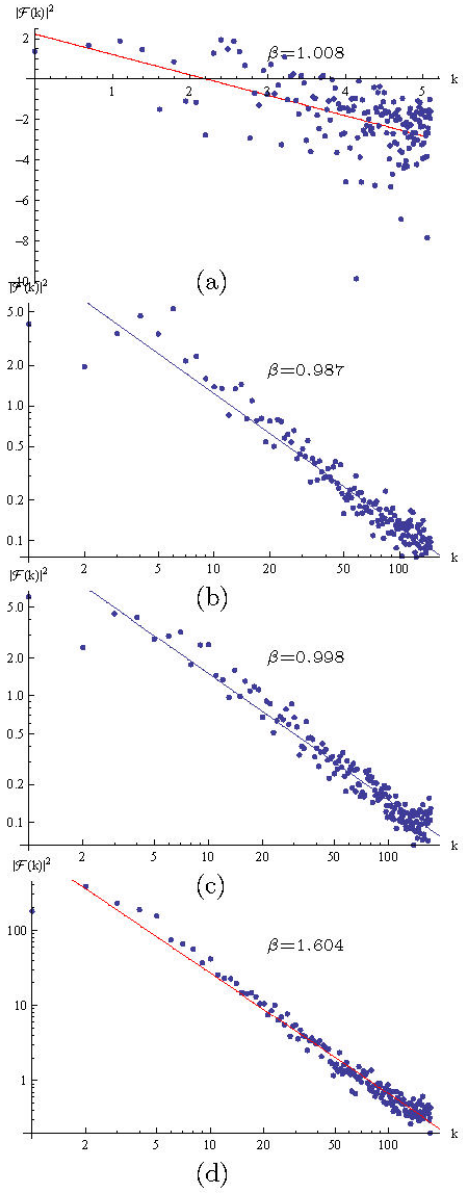


FIGURE 5. Linear fit of the Power Spectrum ($\log |\mathcal{F}_k|^2$ vs $\log k$) of the energy fluctuations in $^{48}$Ca ($J^\pi = 0^+$ subspace) obtained with (a) a realistic interaction, (b) with angular momentum-preserving random interactions (TBRE), and with RMT ensembles (c) GOE and (d) GDE. Here $|\mathcal{F}_k|$ is the Fourier amplitude corresponding to the frequency $k$ in the discrete Fourier transform of the time series.

natural to expect a similar behavior as in Fig. 4b for larger subspaces.

In Ref 11 Relaño *et al.* performed the first study of the behavior of the power spectrum of the energy fluctuations of TBRE random shell model calculations for $^{24}$Mg and $^{32}$Na and found that they obey a $1/f$ scaling. Our own power spectrum calculations of the energy fluctuations in the subspace $J^\pi = 0^+$ of the spectrum of $^{48}$Ca Fig. 5b shows a behavior similar to the one obtained by Relaño *et al.* Ref. 11. Energy fluctuations in TBRE calculations are characterized by a reduction of the spreading of the Fourier amplitudes in the power spectrum. This is an advantage of the averaging procedure. The power spectrum fit is shown in Fig. 5b where it can be seen that in this case the linear fit in the log-log plot adequately describes the $1/f^\beta$ behavior of the power spectrum. A different situation was observed in the case of the corresponding shell model calculations with realistic interactions depicted in Fig 5a. The value obtained for the scaling exponent was $\beta = 0.99$ (see Table II) which implies a scale invariance of the energy fluctuations in the TBRE calculations.

TABLE II. Comparison between shell model calculations with (a) realistic interactions, (b) random interactions (TBRE) and (c) GOE calculations in the spectrum subspace $J^\pi = 0^+$ of $^{48}$Ca.

| | | $\alpha$ | $\beta$ |
|---|---|---|---|
| $^{48}$Ca , $J^\pi = 0^+$ | (Shell Model) | 0.969 | 1.008 |
| | (TBRE) | 1.003 | 0.987 |
| GOE | $N = 347$ | 0.951 | 0.998 |
| | $N = 1000$ | 0.942 | 1.069 |
| GDE | $N = 347$ | 1.338 | 1.604 |
| | $N = 1000$ | 1.398 | 1.786 |

### 5.3. GOE

For comparison purposes we applied the DFA method to the energy fluctuations in the case of GOE. In order to make a fair comparison we considered a GOE with the same dimension as the case of the subspace $J^\pi = 0^+$, where both types of shell model calculations (with realistic and random interactions) were used. A set of 25 matrices in the ensemble was used. The energy fluctuations represented by the time series $\delta_n$ and its integrated form $\psi_n$ are shown in Fig. 2c and Fig. 3c respectively. With the results of the DFA analysis we obtained a value for the self similarity parameter $\alpha = 0.95$ (see Table II), consistent with $\alpha = 1$. This 5% deviation from the expected value $\alpha = 1$ is probably due to the unfolding procedure used in the analysis. This is also suggested by the fact that in larger GOE calculations with a dimension $N = 1000$ a similar deviation from the value $\alpha = 1$ is observed. It is important to recall that in the limit $N \to \infty$, the cumulative function $N(E)$ follows a semicircular law. However, even for the case $N = 1000$ we observe significant deviations. For the time being appropriate unfolding will be discussed elsewhere [14].

The corresponding power spectrum calculations, on the other hand, give a scaling exponent $\beta = 0.998$ (see Table II). It seems that in this case the power spectrum approaches the value 1 more than the DFA method, although we should verify this for a more ample choice of matrix dimensions. In Fig. 4c and 5c we show the averaged results for the DFA and the averaged power spectrum calculations, respectively, for the energy fluctuations in the GOE spectrum with 347 levels using an ensemble with 25 sets.

### 5.4. GDE

Finally, and for the sake of completeness, we applied the DFA method to the case of the integrable GDE random ensemble. Again we used the same dimension as the case of the subspace $J^\pi = 0^+$. The energy fluctuations represented by the time series $\delta_n$ and its integrated form $\psi_n$ are shown in Fig. 2d and 3d, respectively. In this case, the uncorrelated nature of the energy fluctuations is noticeable in those figures. The self similarity parameter was calculated by an averaging procedure over the DFA results (Fig. 4d), and it was found to be $\alpha = 1.34$. This value has a deviation of $\sim$20% from the expected value of $\alpha = 3/2$ (corresponding to uncorrelated time series), although for larger dimensions, *e.g.*, for $N = 1000$, the value for the $\alpha$ parameter was $\alpha = 1.40$, which is closer to the expected value. On the other hand, the scaling exponent in the power spectrum was found to be $\beta = 1.60$, which also deviates $\sim$ 20% from the expected value of $\beta = 2$ for the case of Poisson distributed data. For a larger dimensionality $N = 1000$, the value for the $\beta$ parameter was $\beta = 1.80$, approaching the expected value. The reason for the above mentioned seems to be due to the polynomial unfolding used in the present study. We must stress the fact that present calculations should be considered as preliminary.

## 6. Conclusions

The DFA technique has been applied to the nuclear spectrum of $^{48}$Ca for different $J^\pi$ states obtained with realistic, and random Shell Model calculations, to study the scaling properties of the energy fluctuations around the regular (equally spaced) spectrum. It was shown that the energy fluctuations in the spectrum of $^{48}$Ca defined by the stochastic sequence (6) exhibit non-trivial scale invariance corresponding to a *critical* value of the self similarity parameter $\alpha \simeq 1$, for which the associated autocorrelation function is statistically scale independent. This result is in agreement with the corresponding power spectrum calculations for which a statistical power-law behavior $\sim 1/f$ is observed. This scaling of the energy fluctuations was observed in both, random shell model (TBRE) calculations, as well as in shell model calculations with realistic interactions. However, the DFA results appear to be more robust than the power spectrum calculations. The linear scaling showed in Figs. 4a-4d manifest this fact. In contrast, the power spectrum calculations depicted in Figs. 5a-5d display a rather large spread in the Fourier amplitudes, specially in the case of shell model calculations with a realistic interaction, giving rise to results which are less transparent. In other cases we require further manipulation of the data, such as averaging over several calculations. The DFA method confirms almost perfect non-trivial statistical scale invariance for high-energy fluctuations in $^{48}$Ca. Critical scale invariance was also observed in the case of GOE. Since this class of scale invariance is observed in several classical chaotic phenomena, as well as in phase transitional critical points (logistic maps, geometrical fractals, dripping faucet experiments, etc.), this result suggests a possible underlying connection between classical and quantum chaos. This is an open question which we shall continue to investigate.

## Acknowledgments

We are grateful to Jose Barea for his many suggestions. We thank H. Larralde for his valuable comments. This work was supported in part by PAPIIT-UNAM and Conacyt-Mexico.

---

*i*. Here, a *regularized* spectrum having $\langle s \rangle = \int_0^\infty s\, P(s)\, ds = 1$, is assumed.

*ii*. One of the signatures of fractal structure is associated to the appearance of energy level repulsion in the quantum spectrum, which leads to the Wigner surmise of RMT.

*iii*. The correlation lenght $\xi$ is related to the behavior of the correlation function $\Gamma(r)$. Near a critical point the correlation function has the Ornstein-Zernike form $\Gamma(r) \sim r^{-p} e^{-r/\xi}$ when $T \to T_{crit}$ (see *e.g.* Ref. 12).

*iv*. For a given time series $\delta_n$, the power spectrum is defined as $S(f) = |\mathcal{F}_f\{\delta\}|^2$, where $\mathcal{F}_f\{\delta\}$ denotes the component of the discrete Fourier transform of $\delta$, having frequency $f$.

*v*. The Wiener-Khinchin theorem establishes that the power spectral density of a random process is the Fourier transform of the corresponding autocorrelation function. For a power spectrum with a power law behavior, the Wienner-Khinchin theorem implies also a power law behavior of the corresponding auto-correlation function.

*vi*. For the time being we assume a finite spectrum with $N$ energy levels.

*vii*. Equivalently, we can make a fit of the density of states function $\rho(E)$, since $\bar{N}(E) \equiv \int_{-\infty}^{E} dE' \bar{\rho}(E')$.

*viii*. First order DFA.

*ix*. For a time series $\delta(i), i = 1, \ldots N$, the autocorrelation function is defined as $\mathcal{C}(\tau) = \sum_{k=1}^{N} \delta(k)\delta(k+\tau)$.

*x*. The criterion used to choose the degree of the polynomial fit was based on the properties of the resulting $\delta_n$-time series, being better for the minimal polynomial degree leading to a time series oscillating around $\delta = 0$ (when not properly done, a straightforward high-degree polynomial fit can even lead to a time series with residual linear tendencies, *i.e.* oscillating around a non-horizontal straight line).

1. M.L. Mehta, *Random Matrices*, 2nd ed. (Academic Press, New York London, 1991).

2. E.P. Wigner, *Results and theory of resonance absorption*, Conference on Neutron Physics by Time-of-Flight, Gatlinburg, Tennessee, 1956.

3. O. Bohigas, M.-J. Giannoni, and C. Schmit, *Phys. Rev. Lett.* **52** (1984) 1.
4. M.V. Berry and M. Tabor, *Level clustering in the regular spectrum, Proc. R. Soc. London A.* **356** (1977) 375.
5. T.A. Brody *Lett. Nuovo Cimiento* **7** (1973) 482.
6. P. Chau, Huu-Tai1, N.A. Smirnova, and P. Van Isacker, *Generalized Wigner surmise for ($2 \times 2$) random matrices*, *J. Phys. A***35** (2002) L199.
7. P. Cvitanovic, *et al.*, *Classical and Quantum Chaos*, e-book (2002).
8. M.C. Gutzwiller, *Periodic orbits and classical cuantization conditions*, *Jour. Math. Phys.* **12** (1971) 343; M.C. Gutzwiller, *Chaos in Classical and Quantum Mechanics* (Springer, New York, 1990).
9. T.P.J. Penna, P.M.C. De Oliveira, J.C. Sartorelli, W.M. Goncalves, and R.D. Pinto, *Long-range anticorrelations and non-Gaussian behavior of a leaky faucet Phys. Rev. E* **52** (1995) R2168.
10. A.L. Goldberger, D.R. Rigney, and B.J. West, *Chaos and fractals in human physiology. Sci Am* **262** (1990) 42.
11. A. Relaño, J.M.G. Gómez, R.A. Molina, J. Retamosa, and E. Faleiro, *Phys. Rev. Lett* **89** (2002) 244102; *Phys. Rev.* **E 66** (2002) 036209; E. Faleiro, J.M.G. Gómez, R.A. Molina, L. Muñoz, A. Relaño, and J. Retamosa, Phys. Rev. Lett **93** (2004) 244101.
12. K. Huang, *Statistical Mechanics*, Second Edition (John-Wiley and Sons, 1987).
13. J. Flores, M. Horoi, M. Muller, and T.H. Seligman, *Phys. Rev. E.* **63** (2001) 026204.
14. E. Landa *et al.* (to be published).
15. C.-K. Peng, *et. al.*, *Mosaic organization of DNA nucleotides*, *Phys. Rev. E* **49** (1994) 1685; C-K Peng, S. Havlin, H.E. Stanley, and A.L. Goldberger, *Chaos* **5** (1995) 82.
16. F.J. Dyson, *J. Math. Phys. V.* **3** (1962) 140; 157; 166; 1199.
17. M.S. Santhanam, N. Jayendra, Bandyopadhyay, and Dilip Angom, *Phys. Rev. E* **73** (2006) 015201.
18. C. Heneghan and G. McDarby, *Phys. Rev. E* **62** (2000) 6103.
19. E.W. Montroll, and M.F. Shlesinger, *The wonderful world of random walks*. In: Nonequilibrium Phenomena II. From Stochastics to Hydrodynamics. Lebowitz JL, Montroll EW, eds. (Amsterdam: North-Holland, 1984) p. 1.
20. A.L. Goldberger, *et al.* Physionet: *Components of a New Research Resource for Complex Physiologic Signals*. Circulation 101(23):e215-e220 [Circulation Electronic Pages; http://circ.ahajournals.org/cgi/content/full/101/23/e215]; 2000 (June 13).
21. T.T.S. Kuo and G.E. Brown, *Nucl. Phys. A* **114** (1968) 241.
22. J.B. French and S.S.M. Wong, *Phys. Lett. B* **23** (1970) 449; S.S.M. Wong and J.B. French, *Nucl. Phys. A* **198** (1972) 188; O. Bohigas and Flores, *J. Phys. Lett. B* **34** (1971) 261.
23. T. Papenbrock and H.A. Weidenmüller, *Rev. Mod. Phys.* **79** (2007) 997.
24. E. Caurier, *computer code ANTOINE*, CRN, Strasbourg (2000); E.Caurier, A.P. Zuker, and A. Poves: in *Nuclear Structure of Light Nuclei far from Stability. Experiment ad Theory*, Proceedings of the Workshop, Obrnai, Ed. G. Klotz (CRN, Strasbourg, 1989).